ELSEVIER

Chemical Engineering Journal 89 (2002) 213–221

Chemical Engineering Journal

www.elsevier.com/locate/cej

Preparation of high surface area $La_{1-x}A_xMnO_3$ (A = Ba, Sr or Ca) ultra-fine particles used for CH_4 oxidation

Yuan Liu*, Haitao Zheng, Jinrong Liu, Tong Zhang

Department of Chemical Engineering, Inner Mongolia Polytechnic University, Huhehaot 010062, PR China

Abstract

Ultra-fine particles of $La_{1-x}A_xMnO_3$ (A = Ba^{2+}, Sr^{2+} or Ca^{2+}, $x \leqslant 0.3$) with high surface area and single perovskite structure were prepared by a Na_2CO_3–NaOH coprecipitation method. The so-prepared ultra-fine particles exhibited high catalytic activity for CH_4 total oxidation. The ultra-fine particles of $La_{1-x}Ba_xMnO_3$ prepared with this method were thermally more stable than $LaMnO_3$ and $La_{1-x}Sr_xMnO_3$, and its surface areas were close to 20 m^2/g after sintering at 1000 °C for 2 h. $La_{1-x}Ba_xMnO_3$ exhibited higher activity for methane total oxidation than $La_{1-x}Sr_xMnO_3$, and among the $La_{1-x}Ba_xMnO_3$ series $La_{0.8}Ba_{0.2}MnO_3$ showed highest activity.

Keywords: Perovskite-type oxides; Ultra-fine particles; Methane oxidation; Catalytic combustion

1. Introduction

Perovskite-type oxides (general formula ABO_3) have been attracting much attention for more than two decades due to their potential commercial applications as catalysts for various reactions: oxidation of CO [1,2] and light hydrocarbons [3–6], combustion of natural gas or CH_4 [7–10] (to control NO_x emission by lowing combustion temperature), reduction of NO and SO_2 [11–13], hydrogenation and hydrogenolysis of hydrocarbons [14], etc. Compared to noble metal catalysts, perovskites are less expensive, thermally more stable and exhibiting comparable catalytic oxidation activity. To date, however, such materials have found very limited applications in place of precious platinum catalysts in industrial pollution abatement and automobile emission control. One of the technical constraints to the use of perovskite catalysts is the inability to produce high surface area materials.

Some methods for preparing perovskite-type oxides with comparably high surface areas have been proposed: decomposition of oxalate, cyanide, citrate or acetate precursors [15,16], freeze drying [17], improved complexation [2], sol–gel–cellulose complexation [18], etc. These methods are characterized by the calcination at a comparatively low temperature, resulting in surface areas between 20 and 50 m^2/g. However, their surface areas decrease to 8 m^2/g, in most cases to under 5 m^2/g, as they are calcined at 1273 K, owing to the sintering of the primary particles. Thus, their catalytic activity is significantly lost at higher temperature. Hibino et al. [19] produced high surface area $La_{0.8}Sr_{0.2}MnO_3$ by vibration mill. When the $La_{0.8}Sr_{0.2}MnO_3$ was treated at 1173 K in air for 1 h, its surface area dropped from 35 to 10 m^2/g. Ng Lee et al. [4,20] prepared high surface area perovskite by partial substitution of La^{3+} with K^+ in $LaMnO_3$, and the surface area of $La_{1-x}K_xMnO_{3-\delta}$ were under 5 m^2/g when sintered at 1173 K for 12 h. An alternative method to increase surface area of perovskites is to impregnate it on support materials such as alumina or cordierite [8,21,22]. However, the solid-state reaction of perovskite components with the support material at elevated temperature is often a serious problem in this method.

The properties of perovskite-type oxides, of general formula ABO_3, depend tightly on the nature of A and B ions and on the valence state of A and B. The A site ions are in general catalytically inactive and influence thermal stability of perovskite, while the transition metal ions at B position are active components. By replacing part of A or B ions with A′ and B′, respectively, it is possible to create or suppress oxygen vacancies on the catalysts. Of the ABO_3 examined, La–Mn system, i.e. $LaMnO_3$ showed high oxidation activities, and most excellent activity was attained by $La_{1-x}Sr_xMnO_3$ [23–26]. Other systems [4,10,20], such as $La_{1-x}A_xMnO_3$ (A: Sr, Ce, Eu or K) also exhibited high oxidation activity. The surface areas of $La_{1-x}A_xMnO_3$ (A: Sr, Ce, Eu or K) are much higher than that of $LaMnO_3$ as sintered at same temperature. Hence we think that A position substitution may be a possible route for producing

* Corresponding author.
E-mail address: liuy@mail.impu.edu.cn (Y. Liu).

1385-8947/02/$ – see front matter © 2002 Elsevier Science B.V. All rights reserved.
PII: S1385-8947(02)00013-X

high surface area perovskites. Among $La_{1-x}A_xMnO_3$ system, $La_{1-x}Ba_xMnO_3$ has been rarely reported.

In this work, we have developed a technique for preparing high surface area $La_{1-x}A_xMnO_3$ (A = Ba, Sr or Ca) ultra-fine particles, and we found that the so-prepared $La_{1-x}Ba_xMnO_3$ ultra-fine particles possessed much higher surface area and more thermally stable, and exhibited much higher oxidation activity than $La_{1-x}Sr_xMnO_3$ when they were treated at 1273 K.

2. Experimental

2.1. Catalyst preparation

Substituted $La_{1-x}A_xMnO_3$ and $LaMnO_3$ perovskites were prepared by coprecipitation method. In the synthesis, $La(NO_3)_3{\cdot}6H_2O$, 50 wt.%$Mn(NO_3)_2$ solution, $Sr(NO_3)_2$, $Ba(NO_3)_2$, $Ca(NO_3)_2$, Na_2CO_3 and NaOH were used. The preparation process was listed in Fig. 1. The amounts of distilled water and ethanol listed in Fig. 1 are for producing 10 g of perovskite oxides. For so-prepared samples, their composition were analyzed with inductively coupled plasma (ICP) atomic emission spectrometry (Perkin Elmer, Plasma 40). The results showed that the composition of metals in the ultra-fine particle were same as the starting solution, indicating the metal ions were completely precipitated. Considering the high pH value of the precipitating process, this result is rational. With such washing and filtration circulation (Fig. 1), ICP results showed that the content of Na^+ in the product of perovskite oxides is under 10 ppm.

2.2. Characterization technique

Specific surface areas were calculated by the BET method from the N_2 adsorption isotherms, recorded at liquid nitrogen temperature on a Micromeritics apparatus model ASAP-2000. Prior to the adsorption measurements, samples were out-gassed at 573 K for 4 h.

Powder X-ray diffraction (XRD) patterns of samples were recorded on Riguku D-Max X-ray diffractometer using Cu Kα radiation. Particle size and texture of samples were investigated at Hitachi H-600 transmission electron microscope (TEM).

X-ray photoelectron spectroscopy (XPS) spectra were obtained with PHI-5600 ESCA system spectrometer equipped with a hemispherical electron energy analyzer and a Mg X-ray anode (1253.6 eV) was used. The pressure in analysis chamber during data acquisition was under 10^{-7} Pa. The analysis area was set at 0.8 mm^2. The high-resolution spectra were recorded with pass energy of 23.5 eV. The survey

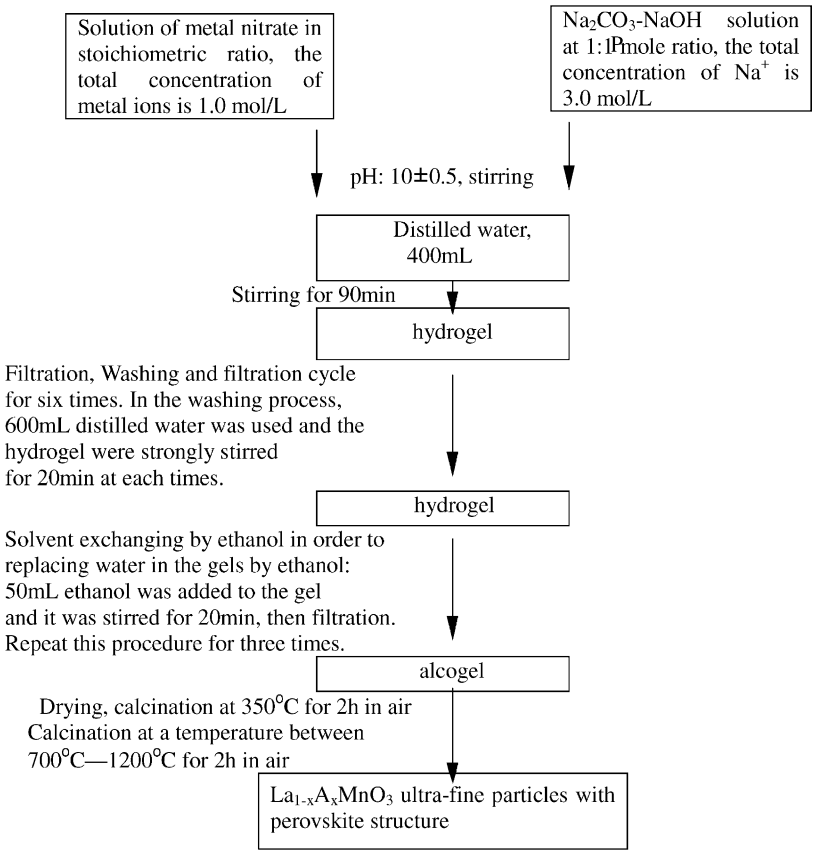

Fig. 1. Preparation procedure of catalysts.

spectra were carried out with pass energy of 187.85 eV. The binding energies (BE) were calibrated with respect to the C 1s value of a contaminated carbon as 284.6 eV. The accuracy of binding energy was estimated to be ±0.2 eV. All the data of spectra were treated using PHI Multipak Version 6.0 software.

2.3. Catalytic activity

The catalytic oxidation of methane was carried out in a fixed-bed quartz tubular reactor (9 mm i.d.) at atmosphere pressure. The 300 (±5) mg of catalysts were used. The reaction mixture was 3.5 vol.% CH_4, 17.0 vol.% O_2 and N_2 to balance, and its space velocity was 20,000 ml/g_{cat} h. The product analysis was accomplished using an on-line gas chromatograph with a TC detector.

3. Results

3.1. X-ray diffraction

The results of XRD phase analysis are listed in Table 1, and its representative profiles are shown in Fig. 2. XRD patterns make possible to monitor not only catalyst structure but also the temperature windows at which the pure perovskite structure is formed. As can be observed, it is possible to obtain pure perovskite structure oxides at 700 °C for $LaMnO_3$ and $La_{0.8}A_{0.2}MnO_3$, while for $La_{0.6}A_{0.4}MnO_3$ and $La_{0.7}A_{0.3}MnO_3$, the calcination temperature of forming pure perovskite structure increase to above 800 °C (see Table 1). It is observable as for substitution ion in $La_{0.6}A_{0.4}MnO_3$ that the larger the ion size is ($Ca^{2+} < Sr^{2+} < Ba^{2+}$) the more difficulty the perovskite structure to be formed.

Table 1
Characteristics of catalysts

Catalysts	Calcination temperature (°C)	Structure[a]	S_{BET} (m^2/g)	Particle size (nm)	$T_{50\%}$ (°C)	$T_{100\%}$ (°C)
$LaMnO_3$	700	s.p.	34.7	25	367	375
	800	s.p.	21.8	35	390	420
	1000	s.p.	1.8	200	600	700
	1200	s.p.	0.15		705	720
$La_{0.8}Ca_{0.2}MnO_3$	700	s.p.	37.6	22	375	390
	800	s.p.	30.3	30	375	390
	1000	s.p.	3.02	150	675	730
	1200	s.p.	0.20		690	750
$La_{0.6}Ca_{0.4}MnO_3$	700	△△	43.0	18	380	445
	800	△	34.6	25	385	400
	1000	s.p.	5.02	180	685	720
	1200	s.p.	0.43		715	750
$La_{0.8}Sr_{0.2}MnO_3$	700	s.p.	32.9	25	355	370
	800	s.p.	28.4	30	365	380
	1000	s.p.	9.69	65	585	650
	1200	s.p.	0.22		710	750
$La_{0.6}Sr_{0.4}MnO_3$	700	△△△	44.2	18	375	390
	800	△△	36.2	20	375	400
	1000	s.p.	7.86	70	500	600
	1200	s.p.	0.47		705	740
$La_{0.9}Ba_{0.1}MnO_3$	700	s.p.	44.8	18	405	420
	800	s.p.	43.8	20	390	410
	1000	s.p.	19.3	40	455	480
	1200	s.p.	1.00		730	740
$La_{0.8}Ba_{0.2}MnO_3$	700	s.p.	47.0	15	365	410
	800	s.p.	36.0	20	365	390
	1000	s.p.	16.7	45	405	420
	1200	s.p.	0.1		700	740
$La_{0.7}Ba_{0.3}MnO_3$	700	△	29.7	25	385	395
	800	s.p.	26.2	30	380	400
	1000	s.p.	12.7	55	410	435
	1200	s.p.	1.15		700	740
$La_{0.6}Ba_{0.4}MnO_3$	700	△△△	30.8	28	380	390
	800	△△	26.2	35	385	400
	1000	△	15.5	45	410	435
	1200	s.p.	2.42		700	740

[a] s.p. stands for single perovskite structure, and △ stands for impurity peaks (the more of △, the stronger of the impurity peak).

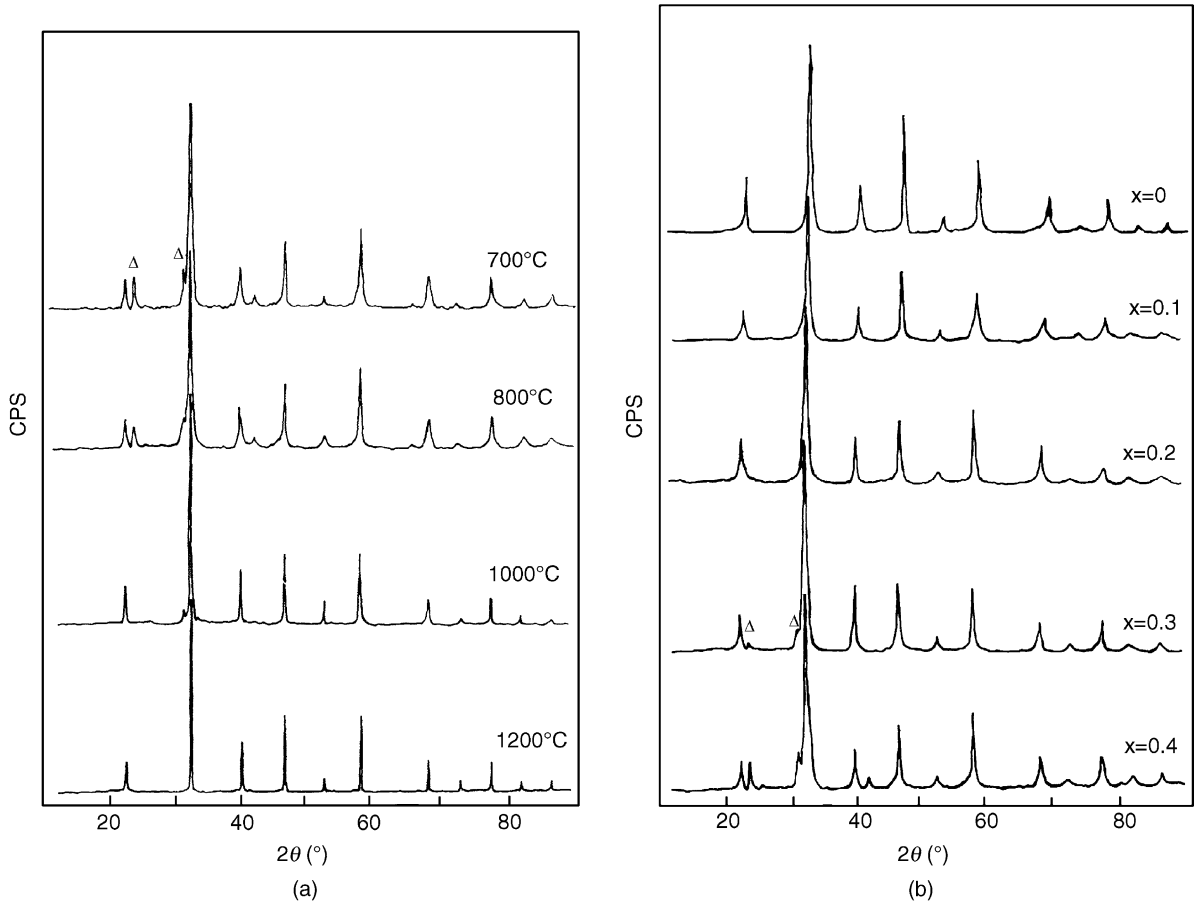

Fig. 2. X-ray diffraction patterns of: (a) $La_{0.6}Ba_{0.4}MnO_3$ calcined at different temperatures and (b) $La_{1-x}Ba_xMnO_3$ catalysts calcined at 700 °C (x: 0–0.4).

It can be seen from Fig. 2(b) that with the increase of x in $La_{1-x}Ba_xMnO_3$, the diffraction peaks move to lower 2θ values, indicating that lattice inter-planar spacing and lattice parameters increase with the increase of Ba^{2+} content, which may be caused by higher ion size of Ba^{2+} in comparison with La^{3+}. The shift of the peak position is also an indicative of the accommodation of Ba^{2+} ions into the lattice structure. Fig. 2(a) shows that crystal size increased (diffraction peaks become narrower) with the increase of calcination temperature.

3.2. TEM and physical adsorption

Representative transmission electron micro-graphs of $La_{1-x}A_xMnO_3$ and $LaMnO_3$ are shown in Fig. 3, and the average particle sizes derived from TEM and specific surface areas of the samples are listed in Table 1. As seen from Fig. 3 and Table 1, partial substitution of La^{3+} in $LaMnO_3$ with Ba^{2+}, Sr^{2+} or Ca^{2+} result in a substantial increase of its specific surface area and a decrease of particle size. Especially for catalysts sintered at comparably high temperature, such as 1000 °C. The specific surface areas of $La_{1-x}A_xMnO_3$ are significantly higher than that of $LaMnO_3$, and the particle sizes of the former are much smaller than that of the latter (for catalysts sintered at 1000 °C). These results indicate that partial substitution of La^{3+} with Ba^{2+}, Sr^{2+} or Ca^{2+} can efficiently elevate the thermal stability of $LaMnO_3$. The specific surface areas of all the samples decreased markedly as the samples are sintered at 1200 °C.

Among the three substitution ions, the Ba^{2+} is most efficiency, and the thermally most stable catalyst is $La_{1-x}Ba_xMnO_3$. The specific surface areas of $La_{0.8}Ba_{0.2}MnO_3$ and $La_{0.9}Ba_{0.1}MnO_3$ calcined at 1000 °C are 16.7 and 19.3 m^2/g, respectively.

3.3. Activity for CH_4 total oxidation

Light-off temperature ($T_{50\%}$) and full conversion temperature ($T_{100\%}$, diffusion become rate controlling step) on the catalysts are presented in Table 1, and representative relationship profiles of CH_4 conversion vs. reaction temperature are shown in Fig. 4. For catalysts sintered at 700 °C, the $T_{50\%}$ and $T_{100\%}$ were varied in a small scale. Except for $La_{0.8}Sr_{0.2}MnO_3$, activity of $LaMnO_3$ is a little higher than the activity of $La_{1-x}A_xMnO_3$. As for catalysts sintered at

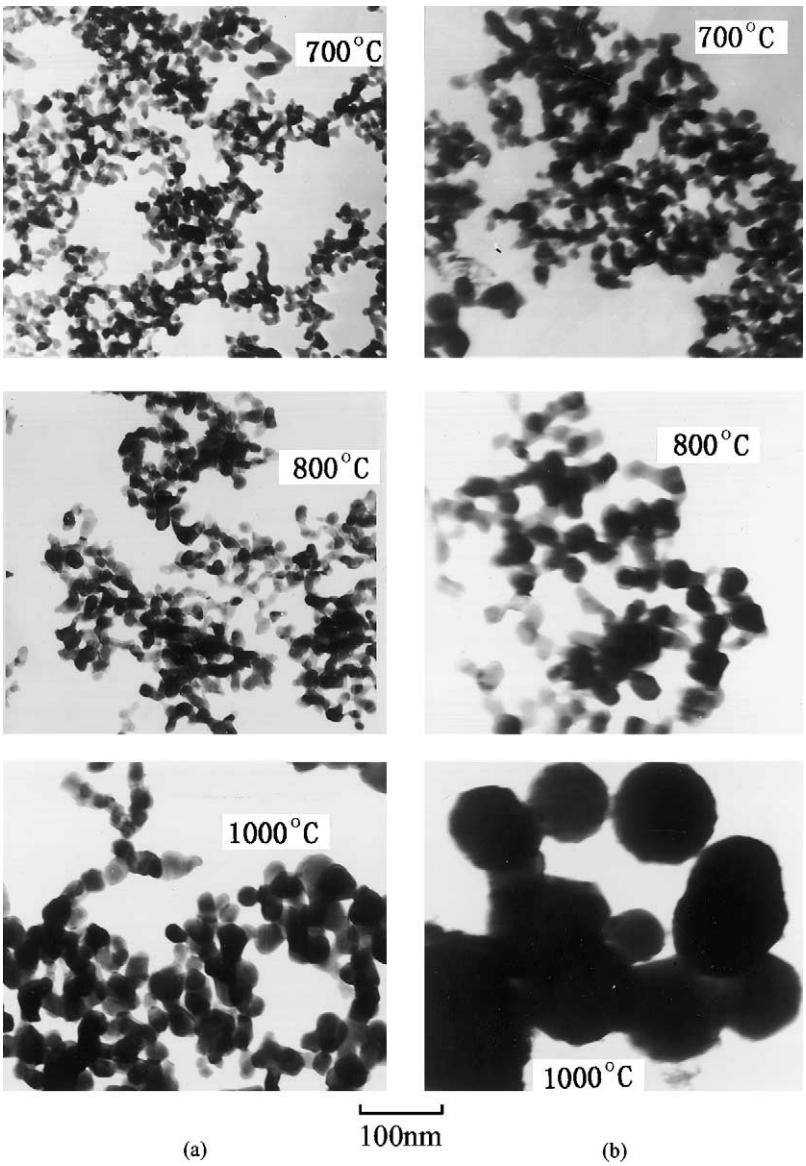

Fig. 3. TEM micrograph of: (a) $La_{0.8}Ba_{0.2}MnO_3$ and (b) $LaMnO_3$ calcined at different temperatures.

800 °C, all of the partial substituted perovskite are more active than $LaMnO_3$. It should be mentioned that full conversion is achieved under 500 °C on $La_{1-x}Ba_xMnO_3$ sintered at 1000 °C, and what is noticeable is that full conversion on $La_{0.8}Ba_{0.2}MnO_3$ sintered at 1000 °C was attained around 420 °C. For the catalysts calcined at 1000 °C, $La_{0.8}Ba_{0.2}MnO_3$ is much more active than $LaMnO_3$ even much more active than $La_{1-x}Sr_xMnO_3$, indicating that $La_{1-x}Ba_xMnO_3$ ultra-fine particles are promising oxidation catalysts.

3.4. XPS

XPS results of $LaMnO_3$ and $La_{0.8}Ba_{0.2}MnO_3$ are presented in Table 2, and representative profiles of XPS are shown in Fig. 5. The binding energies of the $Mn2p_{3/2}$ level of α-Mn_2O_3 and β-MnO_2 are 641.20 and 642.40 eV, respectively [27]. The binding energies of $Mn2p_{3/2}$ presented in Table 2 are close to 641.20 eV, indicating that manganese element is mainly in Mn^{3+} state. The features of $Mn2p_{3/2}$ peaks for $La_{1-x}Ba_xMnO_3$ are broad and asymmetric (Fig. 5b). The covalent character of manganese ground state can result in the broad of the Mn2p3/2 peak [28]. As to the asymmetry, an asymmetric index β was introduced, where β was defined as the ratio of half-width at half-maximum on a high-binding-energy side, W_H, to half-width at half-maximum on a low-binding-energy side, W_L [28]. For $LaMnO_3$ sintered at various temperatures, their β are close to 1.0, while for the series of $La_{0.8}Ba_{0.2}MnO_3$, their β are around 1.3. These results should be the evidence

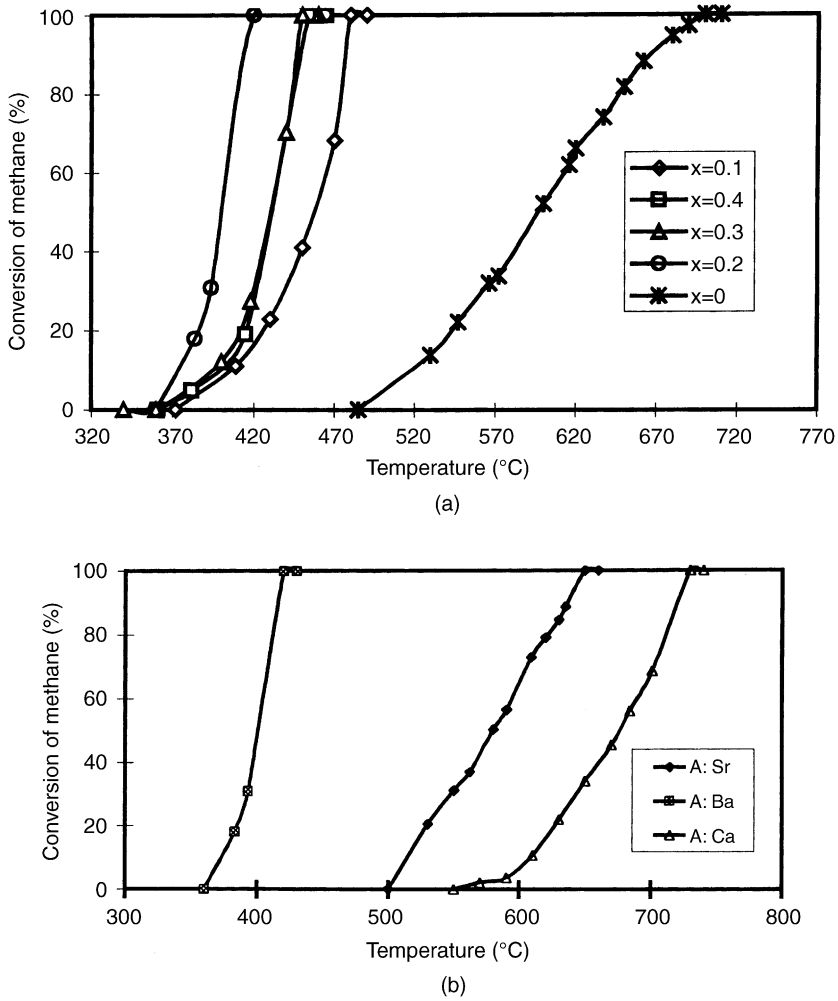

Fig. 4. Light-off temperature curves for the oxidation of methane over: (a) $La_{1-x}Ba_xMnO_3$ and (b) $La_{0.8}A_{0.2}MnO_3$, both were calcined at 1000 °C under 20,000 ml/g_{cat} h and in 3.5 vol.% CH_4, 17.0 vol.% O_2 and N_2 balance.

Table 2
XPS results

Catalysts	Calcination temperature (°C)			
	700	800	1000	1200
$LaMnO_3$				
BE ($La3d_{5/2}$) (eV)	834.1	834.1	834.2	834.6
BE ($Mn3p_{3/2}$) (eV)	641.5	641.5	641.5	641.2
BE ($Ba3d_{5/2}$) (eV)				
Mn (%)[a]	57.8	57.8	60.0	62.8
La (%)[a]	42.2	42.2	40.0	37.2
Ba (%)[a]				
$La_{0.8}Ba_{0.2}MnO_3$				
BE ($La3d_{5/2}$) (eV)	833.8	833.9	834.0	834.5
BE ($Mn3p_{3/2}$) (eV)	641.6	641.5	641.6	641.5
BE ($Ba3d_{5/2}$) (eV)	779.5	779.8	779.6	779.7
Mn (%)[a]	60.8	59.0	60.5	58.9
La (%)[a]	25.9	26.0	24.3	23.1
Ba (%)[a]	13.3	15.0	15.2	13.2

[a] Atomic ratio on catalysts surface.

of the change of the valence state of manganese element from Mn^{3+} to Mn^{4+} in $La_{0.8}Ba_{0.2}MnO_3$.

The binding energies of La3d of $La_{0.8}Ba_{0.2}MnO_3$ shifted to lower value compared to that of $LaMnO_3$, indicating decrease of ionicity of La–O bonds. This phenomenon may be resulted from the change of part of Mn^{3+} to Mn^{4+} as La^{3+} was partially replaced by divalent Ba^{2+}. In Table 2, we see an increase in binding energy of La3d with increase of sintering temperature (i.e. decrease of surface area and increase of particle size). This could be explained by the decrease of dangling bond numbers on the surface (with increase of particle size) resulting in increase of ionicity of La–O bonds. The binding energies of Ba3d of $La_{0.8}Ba_{0.2}MnO_3$ are changed a little for all the samples.

The manganese segregation is observed throughout the samples and the manganese segregation is higher in $La_{0.8}Ba_{0.2}MnO_3$ than in $LaMnO_3$. As for $LaMnO_3$, the surface content of manganese increases with the increase of sintering temperature. The Ba^{2+} ion is segregated on surface in $La_{0.8}Ba_{0.2}MnO_3$ series.

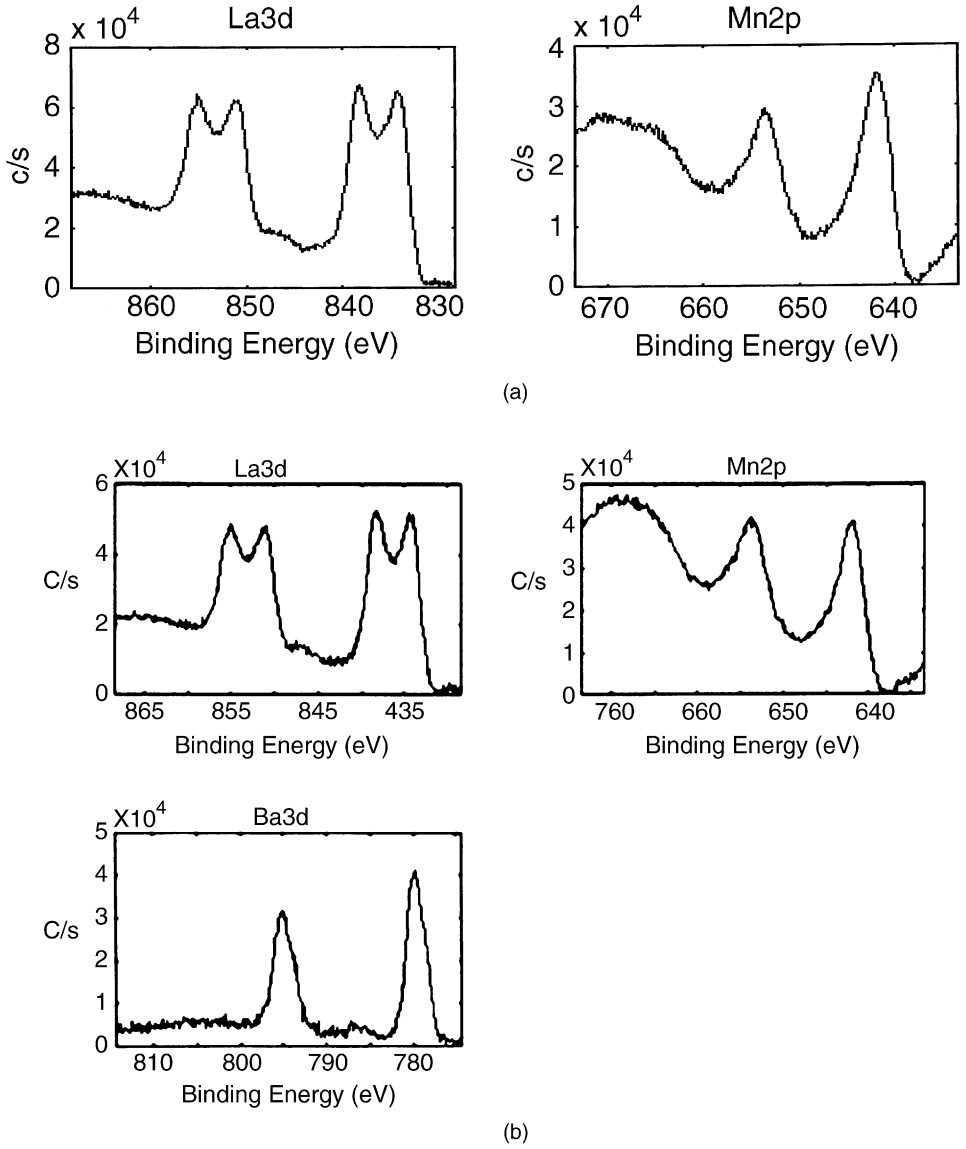

Fig. 5. Typical X-ray photoelectron spectra of: (a) $LaMnO_3$ and (b) $La_{0.8}Ba_{0.2}MnO_3$ calcined at 1000 °C.

4. Discussion

Single perovskite structure was formed for $La_{1-x}Sr_xMnO_3$ ($x \leqslant 0.3$) when the samples were sintered at 700 °C for 2 h through Na_2CO_3–NaOH-coprecipitation method, while in synthesizing $La_{1-x}Sr_xMnO_3$ through coprecipitation method [$(NH_4)_2CO_3$, NH_4OH or NaOH as precipitating agent] the sintering temperature for obtaining a single perovskite phase were generally higher than 850 °C [19,26,29]. When the precipitating agent was changed to NaOH or Na_2CO_3 solution, single perovskite structure could not be formed at the same sintering condition. These results indicate that the Na_2CO_3–NaOH precipitating agent allow the components of these metal ions to be uniformly dispersed in the precursors, which decreased the activation energy of the solid state reaction in the perovskite structure forming process.

Alcohol washing before drying has a significant effect on the morphology and texture properties of zirconia and alumina [30,31], which have been rationalized in mainly two ways. Alcohol washing could reduce capillary forces within the precipitate as a result of lowing the surface tension, thus leading to less pore collapse during the subsequent drying or calcination. The second effect of alcohol washing is a steric inhibition between primary particles as a result of hydrogen bonding of ethanol to surface hydroxyl groups, thus inhibiting inter-particle poly-condensation reactions in the gel-drying procedure, which would lead to increase of particle sizes. In our experiment, alcohol washing effectively inhibited the particle aggregation of the perovskite-type oxide precursors.

The specific surface areas of $La_{1-x}A_xMnO_3$ are much higher than that of $LaMnO_3$ as sintered at 800 °C, especially at 1000 °C, indicating partial substitution of La^{3+} with Ba^{2+},

Sr^{2+} or Ca^{2+} effectively elevate the thermal stability of the perovskite-type oxides, and the Ba^{2+} is the most effective substitution ion among the three. The Ba^{2+} ions were segregated towards the surface as can be seen in Table 2. Surface content of Ba^{2+} increased with sintering temperature, except for sintering temperature of 1200 °C (at so high a temperature, well-dispersed BaO particles might be formed). For the series of $La_{1-x}Sr_xMnO_3$, surface segregation of Sr^{2+} has been reported [32,33], and the surface segregation increased with sintering temperature. The surface segregation of Ba^{2+} and Sr^{2+} indicates that the system is more stable as Ba^{2+} or Sr^{2+} ions is migrated on to the surface, in another words, the migration of Ba^{2+} or Sr^{2+} from surface to bulk is not favored, especially for Ba^{2+}. This should be leaded by the large ion size of Ba^{2+}. The ion radii of Ba^{2+}, Sr^{2+}, Ca^{2+} and La^{3+} are 1.34, 1.12 0.99 and 1.01 Å, respectively. The process of particle growth and agglomeration are accompanied by inter-particle sintering, i.e. neck-formation and growth, which resulted from migration of ions from surface to bulk [31]. Hence, the Ba^{2+} or Sr^{2+} segregated on the surface formed an inhibiting layer for the neck-forming and growth, and thus their thermal stability was improved. The surface areas of $La_{1-x}Ba_xMnO_3$ are close to 20 m^2/g even after sintered at 1000 °C (Table 1).

The catalytic activities of methane oxidation on $La_{1-x}Ba_xMnO_3$ series were found to increase with the increase in surface area [33]. The chemically adsorbed oxygen was increased with the increase of the surface area of $La_{1-x}Sr_xMnO_3$ [33], and CH_4 combustion on $La_{1-x}Sr_xMnO_3$ is supra-facial reaction hence adsorbed oxygen played an important role [24]. The substitution of La^{3+} with divalent Sr^{2+} lead to the change of part of Mn^{3+} to Mn^{4+} and to the formation of highly oxidative compound $La_{1-x}Sr_xMnO_{3+\delta}$. Both of them elevated its catalytic activity. For the $La_{1-x}Ba_xMnO_3$ series, shift of Mn^{3+} to Mn^{4+} was observed by XPS, and the binding energy of La3d changed to lower values compared to La3d in $LaMnO_3$, on the other side, segregation of manganese ions and Ba^{2+} to surface were observed. These changes of surface structure and composition will make a significant effect on catalytic activity.

5. Summary

With the Na_2CO_3–NaOH-coprecipitation method, high surface area ultra-fine particles of $La_{1-x}A_xMnO_3$ (A: Ba^{2+}, Sr^{2+} or Ca^{2+}, $x \leqslant 0.3$) in single perovskite structure can be made. The so-prepared ultra-fine particles exhibited high catalytic activity for CH_4 total oxidation. In the preparing process, the precipitating agent of Na_2CO_3–NaOH leaded uniformly distributed precursors and the ethanol washing could effectively inhibit the particle aggregation in the gel-drying process. The partial substitution of La^{3+} in $LaMnO_3$ with Ba^{2+} or Sr^{2+} resulted in the modification of surface properties of the particles, which significantly increased the thermal stability and catalytic activity of the perovskite oxides. The results showed that the ultra-fine particles of $La_{1-x}Ba_xMnO_3$ prepared with this method are thermally much more stable and more active for methane total oxidation than $LaMnO_3$ and $La_{1-x}Sr_xMnO_3$.

Acknowledgements

Financial support from Chinese National Natural Science funds (No. 29869001) is gratefully acknowledged. Thanks are due to Dr. Q.S. Liu for fruitful help in the investigation of catalytic activities. Thanks are due to Mrs. Fei He for her work on XPS.

References

[1] B. Viswanathan, CO oxidation and NO reduction on perovskite oxides, Catal. Rev. Sci. Eng. 34 (1992) 337.
[2] J. Shu, S. Kaliaguine, Well-dispersed perovskite-type oxidation catalysts, Appl. Catal. B 16 (1998) L303.
[3] T. Seiyama, Total oxidation of hydrocarbon on perovskite oxides, Catal. Rev. Sci. Eng. 34 (1992) 281.
[4] Y. Ng Lee, Z. El-Fadli, F. Sapina, E. Martinez-Tamayo, V. Corberan, Synthesis and surface characterization of nanometric $La_{1-x}K_xMnO_{3+\delta}$ particles, Catal. Today 52 (1999) 45.
[5] G. Sinquin, J.P. Hindermann, C. Petit, A. Kiennemann, Perovskites as polyvalent catalysts for total destruction of C_1, C_2 and aromatic chlorinated volatile organic compounds, Catal. Today 54 (1999) 107.
[6] V.R. Choudhary, S. Banerjee, B.S. Uphade, Activation by hydrothermal treatment of low surface area ABO_3-type perovskite oxide catalysts, Appl. Catal. A 197 (2000) L183.
[7] D. Ferri, L. Forni, Methane combustion on some perovskite-like mixed oxides, Appl. Catal. B 16 (1998) 119.
[8] S. Cimino, L. Lisi, R. Pirone, G. Russo, M. Turco, Methane combustion on perovskites-based structured catalysts, Catal. Today 59 (2000) 19.
[9] H. Arai, T. Yamada, K. Eguchi, T. Seigama, Catalytic combustion of methane over various perovskite-type oxides, Appl. Catal. 26 (1986) 265.
[10] L. Marchetti, L. Forni, Catalytic combustion of methane over perovskites, Appl. Catal. B 15 (1998) 179.
[11] K. Tabata, M. Misono, Elimination of pollutant gases—oxidation of CO, reduction and decomposition of NO, Catal. Today 8 (1990) 249.
[12] Y. Teraoka, H. Nii, S. Kagawa, K. Janson, M. Nygren, Influence of the simultaneous substitution of Cu and Ru in the perovskite-type (La, Sr)MO_3 M = Al, Mn, Fe, Co on the catalytic activity for CO oxidation and CO–NO reductions, Appl. Catal. A 194 (2000) 35.
[13] J. Ma, M. Fang, N. Lau, The catalytic reduction of SO_2 by CO over lanthanum oxysulphide, Appl. Catal. A 150 (1997) 253.
[14] K. Ichimura, Y. Inoue, I. Yasumori, Hydrogenation and hydrogenolysis of hydrocarbons on perovskite oxides, Catal. Rev. Sci. Eng. 34 (1992) 301.
[15] G. Saracco, F. Geobaldo, G. Baldi, Methane combustion on Mg-doped $LaMnO_3$ perovskite catalysts, Appl. Catal. B 20 (1999) 277.
[16] J.M.D. Tascon, S. Mendioroz, L.G. Tejuca, Preparation, characterization and catalytic properties of $LaMeO_3$, Z. Phys. Chem. Neue Folge 124 (1981) 109.
[17] J. Kirchnerova, D. Klvana, J. Vaillancourt, J. Chaouki, Evaluation of some cobalt and nickel-based perovskites prepared by freeze-drying as combustion catalysts, Catal. Lett. 21 (1993) 77.
[18] Z.P. Shao, G.X. Xiong, S.S. Sheng, H.R. Chen, L. Li, New methods to prepare perovskite-type $La_{0.8}Sr_{0.2}CoO_3$ catalyst at low temperature, Stud. Surf. Sci. Catal. 118 (1998) 431.

[19] T. Hibino, K. Suzuki, K. Ushiki, Y. Kuwahara, M. Mizuno, Ultra-fine grinding of $La_{0.8}Sr_{0.2}MnO_3$ oxide by vibration mill, Appl. Catal. A 145 (1996) 297.
[20] Y. Ng Lee, F. Sapina, E. Martinez, J.V. Folgado, V. Cortes Corberan, Catalytic combustion of ethane over high surface area $Ln_{1-x}K_xMnO_3$ (Ln = La, Nd) perovskites: the effect of potassium substitution, Stud. Surf. Sci. Catal. 110 (1997) 747.
[21] N. Mizuno, Supported perovskites, Catal. Today 8 (1990) 221.
[22] P.E. Marti, M. Maciejewski, A. Baiker, Methane combustion over $La_{0.8}Sr_{0.2}MnO_{3+x}$ supported on MAl_2O_4 (M = Mg, Ni, and Co) spinels, Appl. Catal. B 4 (1994) 225.
[23] J.L.G. Fierro, Structure and composition of perovskite surface in relation to adsorption and catalytic properties, Catal. Today 8 (1990) 153.
[24] N. Yamazoe, Y. Teraoka, Oxidation of perovskites—relationships to bulk structure and composition (valency, defect, etc.), Catal. Today 8 (1990) 175.
[25] J.O. Petunchi, E.A. Lombardo, The effect of bulk and surface reduction upon the catalytic behavior of perovskite oxides, Catal. Today 8 (1990) 201.
[26] X.L. Cui, Y. Liu, New methods to prepare ultra-fine particles of some perovskite-type oxides, Chem. Eng. J. 78 (2000) 205.
[27] J.Q. Wang, W.H. Wu, D.M. Feng, Introduction to electron spectroscopy, Guo Fang Chu Ban She (1992) 537 (in Chinese).
[28] K. Tabata, Y. Hirano, E. Suzuki, XPS studies on the oxygen species of $LaMn_{1-x}Cu_xO_{3+\lambda}$, Appl. Catal. A 170 (1998) 245.
[29] K.S. Chen, J. Ma, S. Jaenicke, G.K. Chuah, J.Y. Lee, Catalytic carbon monoxide oxidation over strontium, cerium and copper-substituted lanthanum manganates and cobaltates, Appl. Catal. A 107 (1994) 201.
[30] P.D.L. Mercera, J.G. van Ommen, E.B.M. Doesburg, A.J. Burggraaf, J.R.H. Ross, Influence of ethanol washing of the hydrous precursor on the textural and structural properties of zirconia, J. Mater. Sci. 72 (1992) 4890.
[31] P.D.L. Mercera, J.G. van Ommen, E.B.M. Doesburg, A.J. Burggraaf, J.R.H. Ross, Zirconia as a support for catalysts—influence of additives on the thermal stability of the porous texture of monoclinic zirconia, Appl. Catal. 71 (1991) 363.
[32] S. Ponce, M.A. Pena, J.L.G. Fierro, Surface properties and catalytic performance in methane combustion of Sr-substituted lanthanum manganites, Appl. Catal. B 24 (2000) 193.
[33] N. Gunasekaran, S. Saddawi, J.J. Carberry, Effect of surface area on the oxidation of methane over solid oxide solution catalyst $La_{0.8}Sr_{0.2}MnO_3$, J. Catal. 159 (1996) 107.